

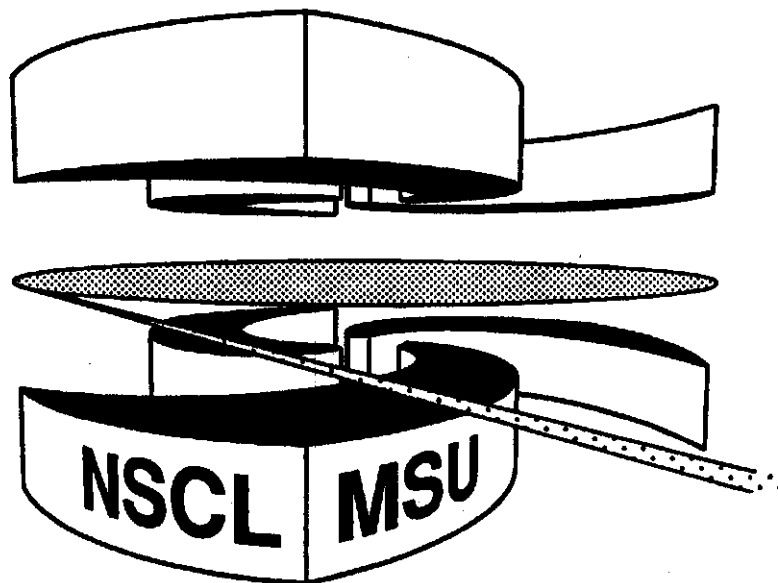


Michigan State University

National Superconducting Cyclotron Laboratory

**THE DYNAMICAL STRUCTURE OF THE Δ -RESONANCE AND
ITS EFFECT ON TWO- AND THREE-NUCLEON SYSTEMS**

G. KORTEMAYER, M.T. PEÑA, P.U. SAUER, and A. STADLER



**The Dynamical Structure of the A-Resonance
and
its Effect on Two- and Three-Nucleon Systems**

G. Kortemeyer

Institut für Theoretische Physik, Universität Hannover, D-30167 Hannover, Germany

and

*NSCL/Cyclotron Laboratory, Michigan State University, East Lansing, MI 48824-1321, U.S.A.**

M. T. Peña

Centro de Física Nuclear da Universidade de Lisboa, P-1699 Lisboa Codex, Portugal

and

Instituto Superior Technico, Lisboa, P-1096 Lisboa Codex, Portugal

P. U. Sauer

Institut für Theoretische Physik, Universität Hannover, D-30167 Hannover, Germany

A. Stadler

College of William and Mary, Williamsburg, VA 23185, U.S.A.+

Abstract

The pion-nucleon interaction in the P_{33} partial wave is assumed to proceed simultaneously through the excitation of the A-isobar and through a phenomenologically introduced non-resonant background potential. The introduction of the background potential allows a more realistic parameterization of the pion-nucleon- Δ vertex compared with the previously used one without

background. It also modifies the propagation of the Δ -isobar in the nuclear medium and gives rise to novel effective nucleon- Δ interactions. Their consequences on predictions for observables in the two-nucleon system at intermediate energies and in the three-nucleon bound state are studied.

I. INTRODUCTION

Internal nucleonic degrees of freedom can get excited when nucleons interact. The lowest state of nucleonic excitation is the Δ ; it decays into pion-nucleon (πN) states. Thus, in nuclear phenomena at intermediate energies Δ -isobar and pion degrees of freedom become active. A hamiltonian describing hadronic and e.m. processes at intermediate energies has to take those degrees of freedom explicitly into account. The Hilbert space to be considered is shown in Fig. 1. Besides the nucleonic sector \mathcal{H}_N , it contains a sector \mathcal{H}_Δ with one nucleon turned into a Δ -isobar and a sector \mathcal{H}_π with one pion added to the nucleons; their projectors are denoted by P_N , P_Δ and Q , respectively. The hamiltonian $H = H_0 + H_1$, to be used to describe the hadronic properties of the two-baryon system with the inclusion of pion production and pion absorption, is diagrammatically defined in Fig. 2; H_0 denotes its kinetic part, H_1 its interaction.

The Δ -isobar, which is introduced in Fig. 1 in the Hilbert sector \mathcal{H}_Δ , is a fictitious baryon of positive parity, spin $\frac{3}{2}$ and isospin $\frac{3}{2}$. A fixed real mass, which is a parameter of the model, and a vanishing width are assigned to it. The Δ -isobar is unobservable, cross sections leading to it are identically zero. In contrast, the physical *resonance* at 1232 MeV in the P_{33} partial wave of pion-nucleon scattering is composed of Δ -isobar and πN states in the model. The hamiltonian models the resonance, which has the physical properties of an effective energy-dependent mass and a non-vanishing energy-dependent width [1], through the $\pi N\Delta$ vertex QH_1P_Δ of Fig. 2(e) and the πN potential QH_1Q of Fig. 2(f).

The modelling of the P_{33} resonance by the hamiltonian is non-unique. E.g., πN scattering up to a mass of 1500 MeV can fully be accounted for under the assumption of a vanishing πN background potential, i.e., with $QH_1Q = 0$. In this case, a mass parameter of $m_\Delta^0 = 1311 \text{ MeV}/c^2$ is assigned to the Δ -isobar; the regularizing cutoff mass for the $\pi N\Delta$ vertex is very small with $\Lambda = 288 \text{ MeV}$; as a consequence, self-energy corrections of the Δ -isobar in the nuclear medium turn out to be quite moderate. The model for the P_{33} resonance without non-resonant background has been used by the authors in the past

[1–4]. This paper introduces an alternative parameterization and explores its consequences for the description of two- and three-nucleon systems: The πN background potential QH_1Q is assumed to be non-vanishing; processes arising from two-pion channels and from meson exchange between pion and nucleon contribute to the background; for simplicity, however, we choose to parametrize the background in a separable form. Furthermore, we require the regularizing cutoff mass Λ for the $\pi N\Delta$ vertex to be of the order of 1 GeV, a magnitude familiar from realistic one-boson exchange two-nucleon potentials; but within that order of magnitude the cutoff mass Λ remains a fit parameter. The fit to P_{33} πN phase shifts determines the parameters in the one-baryon part of the hamiltonian H . E.g., the mass parameter of the Δ -isobar becomes with $m_\Delta^0 = 1801$ MeV/ c^2 quite different from the value for the resonance position of the physical P_{33} resonance. Thus, self-energy corrections of the Δ -isobar in the nuclear medium get dramatically large as will be demonstrated later on.

Sect. II describes the two different models for the P_{33} πN resonance. Different parameterizations for the hamiltonian H of Fig. 2 result. Consequences arising from the different parameterizations of the hamiltonian on predictions for properties of the two-nucleon system above pion threshold are explored in Sect. III; consequences for the three-nucleon bound state are explored in Section IV. Sect. V sums up the conclusions.

II. MODELS FOR THE P_{33} PION-NUCLEON RESONANCE

This section describes P_{33} πN scattering in the framework of the hamiltonian defined in Fig. 2. It assumes that the πN background potential of Fig. 2(f) may not be zero. The considered πN hamiltonian has the following parts, i.e., the kinetic energy H_0 , the $\pi N\Delta$ vertex QH_1P_Δ and the πN potential QH_1Q . The one-baryon nature of the operators is made explicit by the notation

$$H_0 = \sum_i [P_N h_0(i) P_N + P_\Delta h_0(i) P_\Delta + Q h_0(i) Q] + Q h_0(\pi) Q, \quad (2.1)$$

$$QH_1P_\Delta = \sum_i Qh_1(i)P_\Delta, \quad (2.2a)$$

$$P_\Delta H_1 Q = [QH_1P_\Delta]^\dagger, \quad (2.2b)$$

$$QH_1Q = \sum_i Qh_1(i)Q \quad (2.3)$$

as in Ref. [4]. The index i denotes the baryon that the respective operator acts on, i.e., the baryon i in the kinetic energy operator, the Δ -isobar in QH_1P_Δ , and the nucleon involved in the πN background interaction.

Eqs. (2.1)-(2.3) remind us that the operators corresponding to Fig. 2 are defined in the Hilbert space of two baryons; in the reduction to the one-baryon process of πN scattering the label i will be omitted. The form (2.3) of QH_1Q is not general, in contrast to the πN background potential, we still assume the NN potential of Fig. 2(g) in the Hilbert sector \mathcal{H}_π to be vanishing. This assumption has no consequences in πN scattering. However, in two- and three-baryon systems, it is a physics approximation, that Ref. [5] finds to be minor.

The hamiltonian yields the following πN transition matrix $Qt(z)Q$ in the P_{33} partial wave,

$$\begin{aligned} Qt(z)Q &= Qt_{BG}(z)Q + \left[1 + Qt_{BG}(z)Q \frac{Q}{z - Q(h_0 + h_0(\pi))Q} \right] \\ &\times Qh_1P_\Delta \frac{P_\Delta}{z - P_\Delta h_0 P_\Delta - P_\Delta h_1 Q \frac{Q}{z - Q(h_0 + h_0(\pi) + h_1)Q} Qh_1P_\Delta} P_\Delta h_1 Q \\ &\times \left[1 + Qt_{BG}(z)Q \frac{Q}{z - Q(h_0 + h_0(\pi))Q} \right], \end{aligned} \quad (2.4a)$$

$$Qt_{BG}(z)Q = Qh_1Q \left[1 + \frac{Q}{z - Q(h_0 + h_0(\pi))Q} Qt_{BG}(z)Q \right]. \quad (2.4b)$$

The resulting transition matrix is a complicated and non-linear superposition of resonant and non-resonant contributions. We identify as its resonant part

$$Qh_1P_\Delta \frac{P_\Delta}{z - P_\Delta h_0 P_\Delta - P_\Delta h_1 Q \frac{Q}{z - Q(h_0 + h_0(\pi) + h_1)Q} Qh_1P_\Delta} P_\Delta h_1 Q$$

$$= Qh_1P_\Delta \frac{1}{z - M_\Delta(z, k_\Delta)c^2 + \frac{i}{2}\Gamma(z, k_\Delta) - \frac{\hbar^2 k_\Delta^2}{2m_\Delta^0}} P_\Delta h_1Q, \quad (2.5)$$

whereas $Qt_{BG}(z)Q$ carries the information on the πN background potential Qh_1Q . Besides the linear background contribution $Qt_{BG}(z)Q$, the background generates dressing for the $\pi N\Delta$ vertex and modifies the Δ -isobar propagator. The operator $\hbar\mathbf{k}_\Delta$ denotes the Δ -isobar momentum. Fig. 3 shows characteristic contributions to the transition matrix $Qt(z)Q$.

Eq. (2.5) defines the effective mass and the effective width of the Δ -isobar needed in πN scattering, but also in the nuclear medium, i.e.,

$$M_\Delta(z, k_\Delta)c^2 = m_\Delta^0c^2 + \operatorname{Re} \left[P_\Delta h_1Q \frac{Q}{z - Q(h_0 + h_0(\pi) + h_1)Q} Qh_1P_\Delta \right], \quad (2.6a)$$

$$\Gamma_\Delta(z, k_\Delta)c^2 = -2 \operatorname{Im} \left[P_\Delta h_1Q \frac{Q}{z - Q(h_0 + h_0(\pi) + h_1)Q} Qh_1P_\Delta \right]. \quad (2.6b)$$

The effective mass and the effective width depend on the energy z available for πN scattering, on the Δ -isobar momentum $\hbar\mathbf{k}_\Delta$ and on the non-resonant background $Qt_{BG}(z)Q$, as is obvious due to the standard decomposition

$$P_\Delta h_1Q \frac{Q}{z - Q(h_0 + h_0(\pi) + h_1)Q} Qh_1P_\Delta = P_\Delta h_1Q \left[\frac{Q}{z - Q(h_0 + h_0(\pi))Q} + \frac{Q}{z - Q(h_0 + h_0(\pi))Q} Qt_{BG}(z)Q \frac{Q}{z - Q(h_0 + h_0(\pi))Q} \right] Qh_1P_\Delta. \quad (2.6c)$$

This paper employs non-relativistic kinematics in Qh_0Q for the nucleon, but relativistic kinematics in $Qh_0(\pi)Q$ for the pion. The $\pi N\Delta$ vertex is parameterized as in [2] to be of the monopole form

$$Qh_1P_\Delta = |f\rangle \quad (2.7a)$$

$$\langle k|f\rangle = \frac{f^*}{m_\pi c} \sqrt{\frac{4\pi}{3}} \frac{1}{(2\pi\hbar)^3} \frac{\hbar^2 k}{\sqrt{2\omega_\pi(k)}} \left(\frac{\Lambda^2 - m_\pi^2 c^2}{\Lambda^2 + \hbar^2 k^2} \right) \quad (2.7b)$$

with f^* as coupling constant and Λ as a regularizing cutoff momentum. m_π denotes the mass of the pion, $\omega_\pi(k) := c\sqrt{\hbar^2 k^2 + m_\pi^2 c^2}$ the energy of the pion. Instead of the coupling constant f^* , the combination

$$\frac{f^2}{4\pi} := \frac{f^{*2}}{4\pi} \left(\frac{\Lambda^2 - m_\pi^2 c^2}{\Lambda^2 + \hbar^2 k^{*2}} \right) \quad (2.7c)$$

of parameters — $\hbar k^*$ being the relative πN momentum at the resonance position, e.g., $1232 \text{ MeV}/c = m_N c + \hbar^2 k^{*2}/(2m_N c) + \omega_\pi(k^*)/c$ with m_N as nucleon mass — represents the effective coupling of 0.306 between resonance and πN states realistically. The πN background potential is chosen to be separable, i.e.,

$$Qh_1Q := \sum_{\alpha=1,2} |g_\alpha\rangle \lambda_\alpha \langle g_\alpha| \quad (2.8a)$$

with

$$\langle k|g_\alpha\rangle := \frac{\hbar k^{*3} c}{\sqrt{k^*}} \frac{k}{(k^2 + \beta_\alpha^2)^2}, \quad (2.8b)$$

where λ_α and β_α are additional free parameters. The hamiltonian is required to account for the experimental P_{33} πN phase shift in the energy region from threshold to 1500 MeV [6]. Table I summarizes the results (KB) of the fitting procedure for the parameters m_Δ^0 , λ_α and β_α . The parameterization (P) without background potential on which the calculations of Refs. [1–4] are based is given for comparison; it is adapted to the parameterization (Pa) by an improved fit in this paper; the adaptation only yields a minute change in m_Δ^0 . Thus, without physics consequences the parameterizations (P) and (Pa) have been used throughout this paper for reference purposes. Fig. 4 shows the good agreement between calculated and measured phase shifts.

Both descriptions of P_{33} πN scattering, i.e., the one without and with πN background potential, account for phase shifts with comparable quality. Fig. 4 demonstrates that differences in the fits are graphically only discernable at larger energies; it also proves that even in the presence of a background potential the Δ -isobar provides the dominant contribution to the physical resonance. The non-resonant component indeed only appears as a background, which justifies our previous approximation $Qh_1Q = 0$ in retrospect. In fact, an expansion of the πN transition matrix in terms of the transition matrix $Qt_{BG}(z)Q$ of the non-resonant potential reproduces phase shifts better than 2% already in first order in the region of the

resonance within its experimental width. This is proof of the comparative weakness of the πN background potential; in fact, the replacement of the background transition matrix by the background potential, i.e., of $Qt_{BG}(z)Q$ by Qh_1Q , is for the phase shifts an excellent approximation, but becomes considerably poorer outside the resonance region; the replacement can yield some deviations for relative momenta of the πN system below 180 MeV/c, but stays within 1% around the resonance position.

According to Table I the increase of the cutoff momentum Λ , responsible for the suppression of the $\pi N\Delta$ vertex with increasing relative momentum according to Eq. (2.7b), leads to an increase of the bare mass m_Δ^0 of the Δ -isobar. This correlation reveals a balance: On one hand, the larger cutoff Λ enlarges the coupling of πN states to the Δ -isobar; on the other hand, the larger Δ -mass makes the same transition energetically less favorable. Despite that balance, a large bare mass for the Δ -isobar is quite worrisome: It yields substantial self-energy corrections for the Δ -isobar propagation, they are displayed in Fig. 5. The variation of the effective Δ -mass $M_\Delta(z, k_\Delta)$ and Δ -width $\Gamma_\Delta(z, k_\Delta)$ with the available energy z gets important when the Δ -isobar and the interacting πN system are imbedded in many-nucleon systems.

III. EFFECTS ON THE TWO-NUCLEON SYSTEM ABOVE PION THRESHOLD

In the two-nucleon system above pion threshold the following processes involving at most one pion are possible, i.e., $NN \rightarrow NN$, $NN \leftrightarrow \pi d$, $NN \rightarrow \pi NN$, $\pi d \rightarrow \pi d$ and $\pi d \rightarrow \pi NN$; the symbol d stands for deuteron. The processes are unitarily coupled. The technique for calculating observables is taken from Ref. [3]; it solves a coupled-channel problem. The coupled channels have two baryons, either two nucleons or one nucleon and one Δ -isobar. The transcription into a coupled-channel problem is exact: The channel with a pion is projected out. However, it signals its presence by an energy-dependent $N\Delta$ interaction $P_\Delta H_{\text{1eff}}(z)P_\Delta$.

Since the pion is produced or absorbed through the Δ , only the nucleon- Δ channel

receives such effective pionic contributions besides the instantaneous ones $P_\Delta H_1 P_\Delta$ of Fig. 2. They have the form

$$P_\Delta H_{1\text{eff}}(z) P_\Delta = P_\Delta H_1 P_\Delta + P_\Delta H_1 Q \frac{Q}{z - Q(H_0 + H_1)Q} Q H_1 P_\Delta, \quad (3.1a)$$

$$\begin{aligned} & P_\Delta H_1 Q \frac{Q}{z - Q(H_0 + H_1)Q} Q H_1 P_\Delta \\ &= \sum_{i,j,k} P_\Delta h_1(i) Q \left[\frac{Q}{z - Q H_0 Q} + \frac{Q}{z - Q H_0 Q} Q t_{BG}(z - h_0(k)) Q \frac{Q}{z - Q H_0 Q} \right] Q h_1(j) P_\Delta \\ & \quad + \mathcal{O}[(Q t_{BG}(z) Q)^2]. \end{aligned} \quad (3.1b)$$

The arising contributions are displayed in Fig. 6. They are of one-baryon and two-baryon nature. The ones without the πN background potentials are shown as processes (a) and (c). Process (b), corresponding to the part $i = j, k \neq i$ in the sum (3.1b), modifies the one-baryon contribution. Process (d), corresponding to $i \neq j$ and $k = j$, and process (e), corresponding to $i = j = k$, modify the effective $N\Delta$ interaction. The processes (b), (d) and (e) of Fig. 6 are computed in this paper and added to the corresponding ones without background in the formalism in Ref. [3] when calculating observables of the two-nucleon system; the separability (2.8a) of the background potential $Q h_1 Q$ simplifies their computation a great deal technically.

Eq. (3.1b) is an expansion of the effective $N\Delta$ interaction up to first order in the πN background transition matrix $Q t_{BG}(z) Q$. Only those first order contributions are retained in the computation; a sample contribution of second order in $Q t_{BG}(z) Q$, not included, is shown in Fig. 6(f). In the case of P_{33} πN scattering, Sect. II discussed the validity of such an expansion in powers of $Q t_{BG}(z) Q$ and found the first order highly satisfactory. It is believed, though it could not be checked, that the validity carries over to the description of the two-nucleon system above threshold.

The distortion of the asymptotic πd states by the background potential is not considered.

Results for sample observables of elastic two-nucleon scattering, of pion-production in the two-proton reaction $pp \rightarrow \pi^+ d$, and of pion-deuteron scattering are shown in Figs. 7 to 9. The parameterization of the hamiltonian in the two-baryon system is the same as

in Ref. [3]; it contains the $N\Delta$ potential based on meson exchange. The dotted lines in all figures represent the results for the parameterization (P) of the πN interaction without P_{33} background potential; the results are only slightly changed with respect to [3] due to an improvement in calculational technique which is described in Ref. [8]. The solid lines represent the results for the new parameterization (KB) containing the background potential and having a larger cutoff momentum Λ and a larger bare Δ -mass m_{Δ}^0 ; the background is included in the propagator of the Δ -resonance according to Fig. 6(b), and as a correction in the pion exchange potential according to Fig. 6(d) and Fig. 6(e); among the latter two corrections, the vertex correction of Fig. 6(d) is found to be the much more important one.

Observables sensitive towards changes of the interaction in the Hilbert sector \mathcal{H}_{Δ} are phase shifts and inelasticities for the 1D_2 partial wave in elastic NN -scattering, since the nucleonic 1D_2 wave is coupled to the 5S_2 $N\Delta$ wave — pion production and pion-deuteron scattering. Fig. 7 shows the 1D_2 phase shifts. The dashed line is added to isolate the effect of the background, it shows the results for (K) of Table I, i.e., for the new parameterization (KB) while omitting the background contribution. A comparison between the dashed and the solid curve can be used to estimate the direct influence of the background, as in Fig. 4 for the P_{33} phase shifts; the P_{33} resonance is sharpened by the changed resonance parameters (KB) compared with (P), but gets broadened by the background potential also in the two-nucleon system. Fig. 8 shows the influence of the background on differential cross sections for $NN \rightarrow \pi d$, Fig. 9 shows the same for $\pi d \rightarrow \pi d$.

For two energies, computations of the 1D_2 phase shift are also performed with the background potential itself instead of its transition matrix, i.e., for the replacement of $Qt_{BG}(z)Q$ by Qh_1Q . The results of both computations are found to differ by less than 1%, a result that is compatible with the small differences between the two corresponding calculations of the πN phase shifts in Sect. II. Nevertheless, the effect of the background on the considered observables is quite sizeable. As Fig. 7 proves, the effect is an indirect one; the background potential changes the bare Δ -mass and the $\pi N\Delta$ vertex parameters, and that change has a large impact on the observables of the two-nucleon system above pion threshold.

For all considered reactions, the introduction of the πN background potential leads by and large to a poorer agreement with experimental data except for the 1D_2 phase shifts. We attribute this sad fact to the dramatically large self-energy corrections which the Δ -isobar receives according to Fig. 5.

IV. EFFECTS ON THE THREE-NUCLEON BOUND STATE

In the first sections of this paper, the Δ -isobar was used as a reaction mechanism for pion scattering, pion production and pion absorption; that reaction mechanism depends on the introduced πN background potential in the P_{33} partial wave. In bound nuclear systems, the explicit Δ -isobar and pion degrees of freedom yield hadronic and electromagnetic nuclear-structure corrections compared with a purely nucleonic description, e.g., effective medium-dependent many-nucleon interactions and currents. As long as the Hilbert sector \mathcal{H}_π with a pion is assumed to be interaction-free, i.e., $QH_1Q = 0$, the effective many-nucleon interactions and currents remain reducible into one- and two-baryon contributions. Clearly, the two-baryon processes of Fig. 6 keep that character even when imbedded in a larger nuclear medium. However, the πN background potential also yields three-baryon contributions which are irreducible in the baryonic Hilbert sectors. Fig. 10 shows examples for the effective three-baryon interaction which arises in the Hilbert sector \mathcal{H}_Δ . Technically, it can be treated in the three-nucleon bound state as any irreducible three-baryon force according to the technique of Ref. [14]. However, such an exact calculation is technically very demanding and may even not be necessary. Sect. II concluded that the πN background is weak and can reliably be treated in perturbation theory. This section develops such an approximation scheme. The calculations will keep only the two-baryon processes of Fig. 6.

The three-nucleon bound state $|B\rangle$ satisfies the following coupled-channel Schrödinger equation, i.e.,

$$\left[(P_N + P_\Delta)H(P_N + P_\Delta) + P_\Delta H_1 Q \frac{Q}{E_T - QHQ} Q H_1 P_\Delta \right] (P_N + P_\Delta)|B\rangle = E_T(P_N + P_\Delta)|B\rangle, \quad (4.1a)$$

$$Q|B\rangle = \frac{Q}{E_T - QHQ} QH_1 P_\Delta P_\Delta |B\rangle, \quad (4.1b)$$

with the normalization condition

$$\langle B|(P_N + P_\Delta + Q)|B\rangle = 1. \quad (4.1c)$$

The exact set of equations (4.1a)-(4.1c) is compared with the approximate one, in which the πN background potential is neglected, i.e., $QH_1Q = 0$. In zeroth order of the πN background the approximate trinucleon binding energy and wave function are $E_T^{[0]}$ and $|B^{[0]}\rangle$, respectively. We use the following steps in order to relate the exact and the approximate eigenvalues

$$E_T = \frac{\langle B|(P_N + P_\Delta)H(P_N + P_\Delta) + P_\Delta H_1 Q \frac{Q}{E_T - QHQ} QH_1 P_\Delta |B\rangle}{\langle B|P_N + P_\Delta|B\rangle} \quad (4.2a)$$

$$E_T \approx \frac{\langle B^{[0]}|(P_N + P_\Delta)H(P_N + P_\Delta) + P_\Delta H_1 Q \frac{Q}{E_T^{[0]} - QHQ} QH_1 P_\Delta |B^{[0]}\rangle}{\langle B^{[0]}|P_N + P_\Delta|B^{[0]}\rangle} \quad (4.2b)$$

$$E_T \approx E_T^{[0]} + \frac{\langle B^{[0]}|P_\Delta H_1 Q \left[\frac{Q}{E_T^{[0]} - QHQ} - \frac{Q}{E_T^{[0]} - QH_0Q} \right] QH_1 P_\Delta |B^{[0]}\rangle}{\langle B^{[0]}|P_N + P_\Delta|B^{[0]}\rangle} \quad (4.2c)$$

The background potential QH_1Q is assumed to change the baryonic wave function components, i.e.,

$$P_N|B\rangle \approx P_N|B^{[0]}\rangle, \quad (4.3a)$$

$$P_\Delta|B\rangle \approx P_\Delta|B^{[0]}\rangle, \quad (4.3b)$$

and the available energy in the effective interaction, i.e.,

$$P_\Delta H_1 Q \frac{Q}{E_T - QHQ} QH_1 P_\Delta \approx P_\Delta H_1 Q \frac{Q}{E_T^{[0]} - QHQ} QH_1 P_\Delta, \quad (4.3c)$$

by very little. The assumptions (4.3a)-(4.3c) yield the step from Eq. (4.2a) to Eq. (4.2b), and only thereby to Eq. (4.2c).

Since the difference propagator $[Q/(E_T^{[0]} - QHQ) - Q/(E_T^{[0]} - QH_0Q)]$ can be expanded in powers of the background transition matrix $Qt_{BG}(z)Q$, the perturbation scheme (4.2c) for the binding energy E_T is ordered according to powers of $Qt_{BG}(z)Q$. The perturbation scheme (4.2c) does not follow from the Ritz variational principle which works with an expansion in powers of the potential Qh_1Q . We note, however, that for relevant available energies z $Qt_{BG}(z)Q \approx Qh_1Q$ as verified in Sect. II for the πN P_{33} phase shifts and in Sect. III for the NN^1D_2 phase shifts and inelasticities, and that $\langle B^{[0]}|(P_N + P_\Delta)|B^{[0]}\rangle \approx 1$; thus, in this approximation the perturbation scheme (4.2c) becomes

$$E_T = E_T^{[0]} + \langle B^{[0]}|P_\Delta H_1 Q \frac{Q}{E_T^{[0]} - QH_0Q} QH_1 Q \frac{Q}{E_T^{[0]} - QH_0Q} QH_1 P_\Delta |B^{[0]}\rangle \quad (4.4)$$

and is therefore almost variational.

This section compares trinucleon results obtained for the two different parameterizations (KB) and (P) of the P_{33} πN resonance with and without πN background potential according to Sect. II and Table I. An exact Faddeev calculation is done for (KB) without background; we identify its results with $|B^{[0]}\rangle$ and $E_T^{[0]}$ of Eq. (4.2c). First-order perturbation theory according to Eq. (4.2c) is then used to obtain an improved result for the triton binding energy. The perturbation calculations include the one- and two-baryon contributions of Figs. 6(b), 6(d) and 6(e), all contributions being of first order in the πN background transition matrix $Qt_{BG}(z)Q$; the three-baryon process of Fig. 10(a) could not be included. However, the validity of the perturbation theory, first order in $Qt_{BG}(z)Q$, could be checked by comparing the perturbative results for the process of Fig. 6(d) with an exact Faddeev calculation; we claim agreement between the exact and perturbative results on the level of numerical accuracy. Among the three processes the one of Fig. 6(e) accounts for less than 1 eV, which is an order of magnitude smaller than the contributions of the other two, being of the order of a few keV.

The obtained results are collected in Table II. It lists the triton binding energy E_T and the wave function probabilities $P_{\mathcal{L}}$, P_Δ and P_π for the nucleonic components of total angular momentum \mathcal{L} and of particular orbital symmetry, for the components with a Δ -isobar, and

for the components with a pion. The rows 2 and 3 give the changes in binding energy due to the considered non-nucleonic degrees of freedom; ΔE_2 is the change due to effective two-nucleon contributions, ΔE_3 is the change due to effective three-nucleon contributions, as defined in Ref. [15].

The parameterization (KB) of the πN interaction with background leads to a tiny decrease of the binding energy compared with the traditional calculation in Ref. [15] based on the parameterization (P) without background. The decrease corresponds to a decrease of both non-nucleonic effects ΔE_2 and ΔE_3 . Their reduction is plausible, since for (KB) compared with (P) the energy difference $(m_\Delta^0 - m_N)c^2$ is more than doubled. Thus, the excitation of the Δ -isobar gets energetically unfavorable. This fact is borne out by the substantial reduction of the trinucleon Δ -probability P_Δ from 1.71% to 1.16%. In contrast, in the parameterization (KB) the decay of the Δ -isobar into πN -states is less inhibited; this is the reason why the probability P_π of pionic components is increased. In fact, from the ratio of P_Δ and P_π one can conclude that in the old parameterization (P) the Δ -resonance in the trinucleon system has about 3% pionic components, however, in the new parameterization (KB) more than 14%. The influence of the background on these values is very small.

V. CONCLUSIONS

The paper compares two parameterizations of the $\pi N P_{33}$ resonance. Both parameterizations are valid practical realizations of the P_{33} πN interaction in a hamiltonian with nucleon, Δ -isobar and pion degrees of freedom; the hamiltonian is diagrammatically defined in Fig. 2. Both parameterizations are valid ones, since they account for the $\pi N P_{33}$ phase shifts in comparable quality as Fig. 4 and Table I prove. The parameterization (P) puts the πN background potential to zero, the parameterization (KB) employs a non-vanishing one. Though the background potential is weak, Δ -isobar parameters are quite different, and, as a consequence, the self-energy corrections of the Δ -isobar in the nuclear medium are of entirely different size, being much larger over a wide range of energies. The latter fact is

demonstrated in Fig. 5.

The two parameterizations of the $\pi N P_{33}$ resonance are compared in their effects on observables of the two-nucleon system above pion threshold and on properties of the three-nucleon bound state. Sensitivity with respect to the parameterizations is clearly seen, but it is less spectacular than expected from the dramatic differences in the self-energy corrections of the Δ -isobar. The inclusion of the background potential often increases the disagreement between experimental data and theoretical prediction, especially for elastic pion-deuteron scattering and for the pion production reaction $pp \rightarrow \pi^+d$. Compared with the case of vanishing background, the mechanism for pion production and pion absorption is obviously weakened in effective strength, a net result arising from two opposing trends:

- The increased effective mass $M_{\Delta}(z, k_{\Delta})$ of the Δ -isobar inhibits the Δ -isobar propagation as energetically less favorable.
- The increased cutoff mass Λ favors the coupling of pion-nucleon states to the Δ -isobar over a wider range of momenta.

In two-nucleon scattering above pion threshold the first trend seems to dominate. In the three-nucleon bound state simultaneous working of both trends is observed: The Δ -isobar probability P_{Δ} in the wave function is decreased, the pion probability P_{π} is increased.

The two parameterizations of the $\pi N P_{33}$ resonance are considered valid ones for pion-nucleon scattering. Possibly, they could be differentiated and one or the other could be ruled out, when applied to the description of electromagnetic pion production and compton scattering on the nucleon. Furthermore, the discouraging poor description of the two-nucleon system above pion-threshold calls for an overall fit of the employed hamiltonian, i.e., also of the two-baryon potentials, to the data of two-nucleon scattering and of the unitarily coupled processes with one pion. We consider this an important, though scarily complicated task.

ACKNOWLEDGMENTS

The results of the paper are based on the Diploma Thesis of G. K. concluded at the University of Hannover in 1993. G. K. thanks A. Valcarce who acquainted him with the techniques for carrying out the calculations of Sect. II and III, and R. W. Schulze who was always open for conceptual questions, and who together with K. Chmielewski provided the code for changing the angular momentum coupling of three-baryon wave functions between different coupling alternatives. This work was funded by the Deutsche Forschungsgemeinschaft (DFG) under Contract No. Sa 247/7-2 and Sa 247/7-3 (A. St.), by the Deutscher Akademischer Austauschdienst (DAAD) under Contract No. 322-inida-dr (T. P.), by the DOE under Grant No. DE-FG05-88ER40435 (A. St.), by JNICT under Contract No. PBIC/C/CEN/1094/92, and by the Studienstiftung des deutschen Volkes (G. K.). The numerical calculations were performed at the Regionales Rechenzentrum für Niedersachsen (Hannover), at the Continuous Electron Beam Accelerator Facility (Newport News), at the National Energy Research Supercomputer Center (Livermore), and at the National Superconducting Cyclotron Laboratory (East Lansing).

REFERENCES

* Present address.

+ Present address: Centro de Fisica Nuclear da Universidade de Lisboa, P-1699 Lisboa
Codex, Portugal

- [1] K. Dreissigacker, S. Furui, Ch. Hajduk and P. U. Sauer, Nucl. Phys. **A375**, 334 (1982)
- [2] H. Pöpping, P. U. Sauer and Zhang Xi-Zhen, Nucl. Phys. **A474**, 557 (1987), and erratum, Nucl. Phys. **A550**, 563 (1992)
- [3] M. T. Peña, H. Garcilazo, U. Oelfke and P. U. Sauer, Phys. Rev. **C45**, 1487 (1992)
- [4] M. T. Peña, P. U. Sauer, A. Stadler and G. Kortemeyer, Phys. Rev. **C48**, 2208 (1993)
- [5] M. T. Peña, H. Garcilazo and P. U. Sauer, Few Body Systems **Suppl 7**, 239 (1994)
- [6] R. Koch and E. Pietarinen, Nucl. Phys. **A336**, 331
- [7] R. A. Arndt, πN data from VPI&SU, 7/93
- [8] A. Valcarce, F. Fernández, H. Garcilazo, M. T. Peña and P. U. Sauer, Phys. Rev. **C49**, 1799 (1994), footnote p. 1810
- [9] R. A. Arndt, L. D. Roper, R. A. Bryan, R. B. Clark, B. J. VerWest and P. Signell, Phys. Rev. **D28**, 97 (1983)
- [10] A. B. Laptev and I. I. Strakovsky, Leningrad Nuclear Physics Institut report, 1985
- [11] R. Gabatuler *et. al.*, Nucl. Phys. **A350**, 253 (1980)
- [12] C. Ottermann, E. T. Boschitz, W. Gyles, W. List and R. Tacik, Phys. Rev. **C32**, 928 (1985)
- [13] O. A. Yakubovsky, Yad. Fiz. **5**, 1312 (1967) [Sov. J. Nucl. Phys. **39**, 1002 (1984)];
P. Grassberger and W. Sandhas, Nucl. Phys. **B2**, 181 (1967)

[14] A. Stadler and P. U. Sauer, Phys. Rev. **C46**, 64 (1993)

[15] Ch. Hajduk, P. U. Sauer and W. Strueve, Nucl. Phys. **A322**, 329 (1979)

TABLES

TABLE I. Parameters of the πN hamiltonian $(P_\Delta + Q)h(P_\Delta + Q)$ resulting from the fits of P_{33} πN phase shifts. The first two columns (P) and (Pa) refer to the hamiltonian without πN background potential, the version (P) was employed in Refs. [1-4]; the columns three and four (KB) and (K) refer to the hamiltonian with πN background, developed in this paper. Column one, labelled (P), repeats the parameters of Ref. [2], obtained under the assumption of a resonance position m_{Rc^2} at 1236 MeV. In column two, labelled (Pa), the hamiltonian is adapted to the improved experimental data of Ref. [6] with a resonance position m_{Rc^2} of 1232 MeV. Column three, labelled (KB), lists the parameters for the hamiltonian of this paper. The last row indicates the quality of the achieved fits by χ^2/N , $N = 28$, with respect to the data of Ref. [6]. Since error bars are not given for the “experimental” phase shifts of Ref. [6], “experimental” uncertainties of 1° are assumed for all of them when calculating χ^2/N . The set of parameters in column four, labelled (K), is only used when in a calculation with the full hamiltonian (KB) the pure resonance contribution to an observable is to be isolated. It reproduces the correct resonance position, though. The parameter set of column four does not constitute a valid parameterization of the hamiltonian by itself, the resulting χ^2/N is very poor, though not outrageously wrong. The dashed line of Fig. 4 reflects that fact.

	Ref. [2] (P)	adapted (Pa)	(KB)	(K)
m_{Rc^2} [MeV]	1236.0	1232.0	1232.0	1232.0
$m_\Delta^0 c^2$ [MeV]	1315.0	1311.0	1801.0	1801.0
Λ [MeV/c]	287.9	287.9	859.36	859.36
$\frac{f^2}{4\pi} \frac{1}{(\hbar c)^3}$	0.306	0.306	0.306	0.306
λ_1 [1/MeV]	0	0	-0.0522	0
λ_2 [1/MeV]	0	0	0.273	0
$\hbar\beta_1$ [MeV/c]	-	-	369.1	-

$\hbar\beta_2$ [MeV/c]	-	-	597.76	-
χ^2/N	10.0	1.7	0.8	76.4

TABLE II. Results for some trinucleon bound state properties. Results, based on the two parameterizations (P) and (KB) of the P_{33} πN interaction, are compared; the results for (P) are identical with those of Ref. [4] labelled $H(1)$ there. The table lists the triton binding energies E_T , binding energy corrections arising von non-nucleonic degrees of freedom in the definition of Ref. [15], ΔE_2 being the binding energy correction of two-baryon nature; and ΔE_3 being the corresponding correction of three-baryon nature. The table also lists the wave function probabilities, i.e., $P_{\mathcal{L}}$ for nucleonic components of total orbital angular momentum $\mathcal{L} = S, P, D$ and of particular orbital permutation symmetry, the probability P_{Δ} for components with a Δ -isobar, and the probability P_{π} for components with a pion. The binding energies in the first two columns result from exact Faddeev calculations, they are correct within 10 keV only, but the last digits in rows E_T , ΔE_2 and ΔE_3 are believed to represent relative changes between the parameterizations correctly. The binding energy correction of first order in $Qt_{BG}(z)Q$ in the third column is derived in perturbation theory according to Eq. (4.2c).

m_{Δ}^0 [MeV/ c^2]	(P)	(KB)	
	1315.0	1801.0	
		zeroth order in $Qt_{BG}(z)Q$	first order in $Qt_{BG}(z)Q$
E_T [MeV]	-7.849	-7.731	-7.730
ΔE_2 [MeV]	0.456	0.376	0.372
ΔE_3 [MeV]	-0.924	-0.726	-0.721
P_S [%]	88.23	88.70	
$P_{S'}$ [%]	1.24	1.27	
P_P [%]	0.08	0.08	
P_D [%]	8.68	8.59	
P_{Δ} [%]	1.71	1.16	
P_{π} [%]	0.06	0.195	

FIGURES

FIG. 1. Hilbert space for the description of nuclear phenomena at intermediate energies. It consists of three sectors: The sector \mathcal{H}_N contains purely nucleonic states; in \mathcal{H}_Δ one nucleon is turned into a Δ -isobar; in \mathcal{H}_π one pion is added. Nucleons will be denoted by narrow solid lines, Δ -isobars by thick solid lines and pions by dotted lines.

FIG. 2. Graphical definition of the employed interaction hamiltonian H_1 for a two-baryon system. The potentials are instantaneous, the dashed lines represent two-particle interactions in contrast to the instantaneous one-baryon vertex process (e). Processes (a)-(d) denote the potentials between baryons; processes (e)-(g) the coupling to and the interaction in the Hilbert sector with a pion. The hermitian adjoint pieces corresponding to processes (b) and (e) are not shown. The defined hamiltonian is an extension of a purely nucleonic one in isospin triplet partial waves; in isospin singlet partial waves only the purely nucleonic process (a) survives.

FIG. 3. Characteristic contributions to the $P_{33} \pi N$ transition matrix. Process (a) is a purely resonant process, it does not contain any background contribution, while process (b) is a pure background interaction. Process (b) is an example of how the background potential contributes to the $P_{33} \pi N$ scattering; it represents a series of processes in which the potential Qh_1Q is to be replaced by the ladder sum of the transition matrixes $Qt_{BG}(z)Q$. The processes (a) and (c) are sample processes contained in the definition (2.5) of Δ -isobar self-energy corrections.

FIG. 4. πN phase shifts in the P_{33} partial wave. The results for different parameterizations of the P_{33} resonance are compared. The diamonds are the experimental data points from [6] used for the fit of this paper; the diagonal crosses represent newer experimental data according to Ref. [7], which, however, are not taken into account for the present work. The parameterization (KB) of this paper for the P_{33} πN interaction with background potential is shown as solid curve. The parameterization (Pa) without background potential is an improvement of the version (P) given in Ref. [2]; it is shown as dotted curve. The dashed line shows the resonance contribution of the parameterization (KB) alone; the corresponding parameters are collectively labelled (K) in Table I; the parameters (K) *do not* constitute a valid parameterization of P_{33} πN scattering by themselves.

FIG. 5. The effective mass $M_{\Delta}(z, k_{\Delta})$ and width $\Gamma_{\Delta}(z, k_{\Delta})$ of the Δ -isobar, as defined in Eqs. (2.6a) and (2.6b), respectively. Their dependence on the available energy z is shown for vanishing Δ -momentum, i.e., for $\hbar k_{\Delta} = 0$. Results for the parameterization (KB) of this paper with a non-vanishing πN background potential and for the adapted parameterization (Pa) with vanishing πN background potential are compared by solid and dotted lines, respectively. The two compared parameterizations have the bare Δ -masses $1801 \text{ MeV}/c^2$ and $1311 \text{ MeV}/c^2$.

FIG. 6. Effective $N\Delta$ interactions. The processes (a) and (b) are of one-baryon nature, the processes (c)-(f) of two-baryon nature. Only the processes (a) and (c) survive in case the background potential is assumed to vanish. The processes (b), (d) and (e) are first order in the background potential Qh_1Q , process (f) of second order. Each of the processes (b), (d)-(f) represents a series of processes in which the potential Qh_1Q is to be replaced by the ladder sum of the transition matrix $Qt_{BG}(z)Q$.

FIG. 7. 1D_2 phase shifts and inelasticities of elastic two-nucleon scattering as a function of the nucleon lab energy. Results for the parameterization (P) without background potential, and for the parameterization (KB) with background potential are shown as dotted and solid curves. The effect of the background potential is mostly indirect: It changes the bare Δ -mass m_Δ^0 and the parameters of the $\pi N\Delta$ vertex. The direct influence of the background potential is omitted in the results of the dashed curve — it is based on the parameterization (KB), but omitting all background contributions. The experimental data are taken from the energy-independent phase shift analysis of Ref. [9].

FIG. 8. Differential cross section for pion production in $pp \rightarrow \pi^+d$ at two proton lab energies as function of the pion scattering angle in the πd c.m. system. Results for the parameterization (KB) with background potential and for the parameterization (P) without background potential are compared as solid and dotted curves. The data are taken from the compilation of Ref. [10].

FIG. 9. Differential cross sections for elastic pion deuteron scattering at two pion lab energies as a function of the pion scattering angle in the πN c.m. system. Results for the parameterization (KB) with background potential and for the parameterization (P) without background potential are compared as solid and dotted curves. The data are taken from Ref. [11,12].

FIG. 10. Examples for the effective three-baryon interaction in the Hilbert sector \mathcal{H}_Δ arising from the πN background potential. The processes (a), (b) and (c) are of first, second and third order in the background potential Qh_1Q . Each of the processes represent a series of processes in which the potential is to be replaced by the ladder sum of the transition matrix $Qt_{BG}(z)Q$. Even in this extended form, the shown five processes represent only the lowest order ones of the Faddeev-Yakubovsky series [13] for four particles interacting through potentials of very restrictive character. NN interactions within the pionic Hilbert sector \mathcal{H}_π are not considered here, even though they would, through processes like process (d) and (e), also give rise to an effective three-baryon interaction in the Hilbert sector \mathcal{H}_Δ ; the appendix of Ref. [4] describes the technical treatment of the disconnected process (d); process (e) is fully connected.

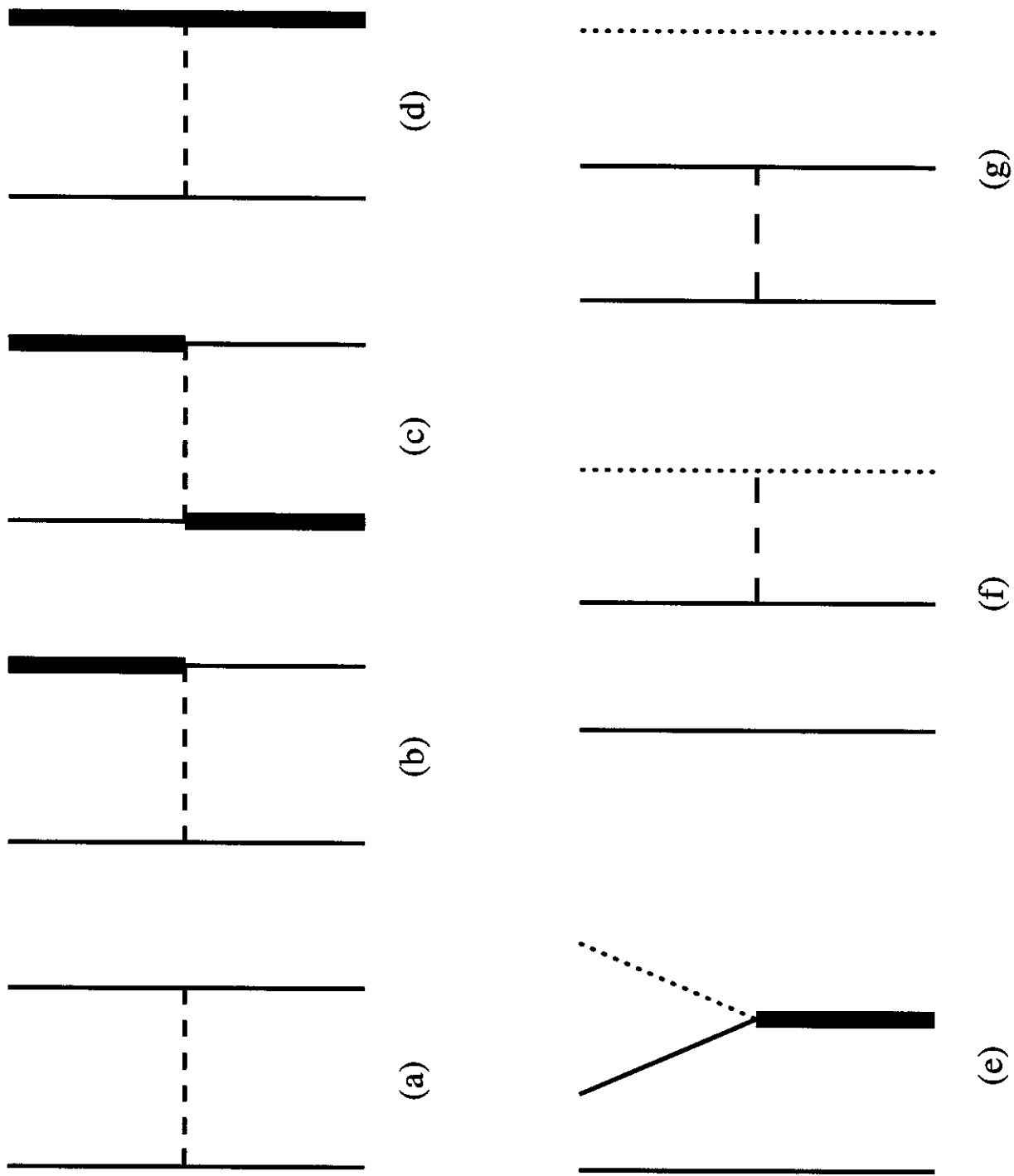


Fig. 2, G.K., P.U.S. : The Dynamical Structure of the Δ -Resonance and its effect on...

Fig 3, Kortemeyer, "The dynamical structure..."

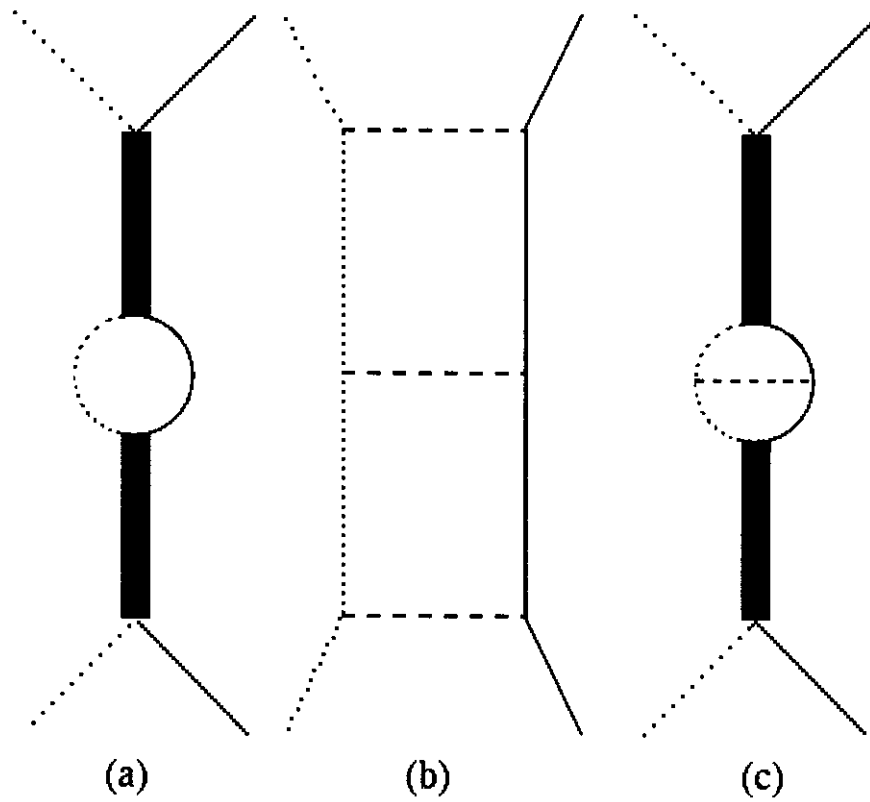


Fig 4, Kortemeyer, "The dynamical structure..."

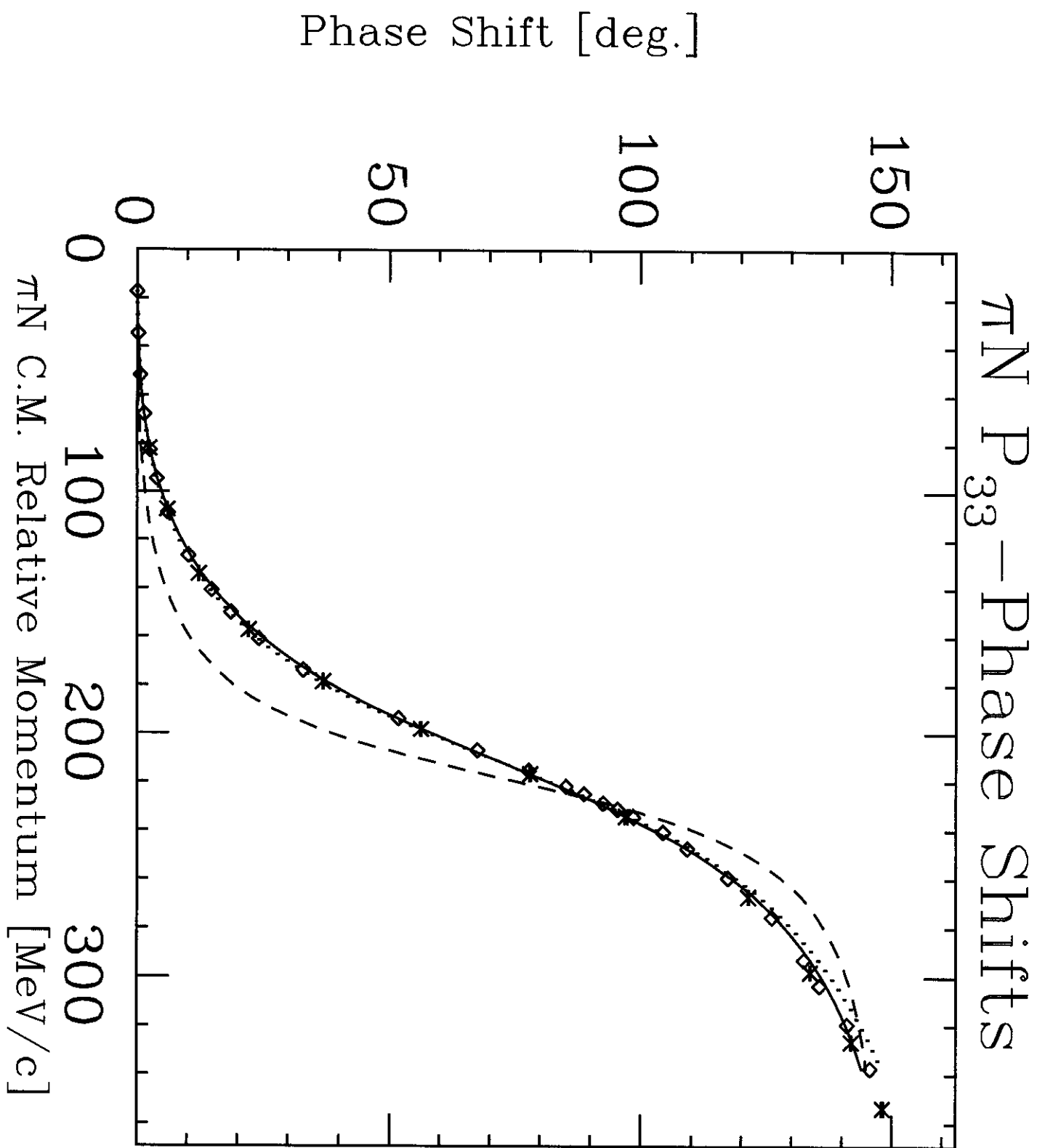


Fig 5, Kortemeyer,
"The dynamical structure..."

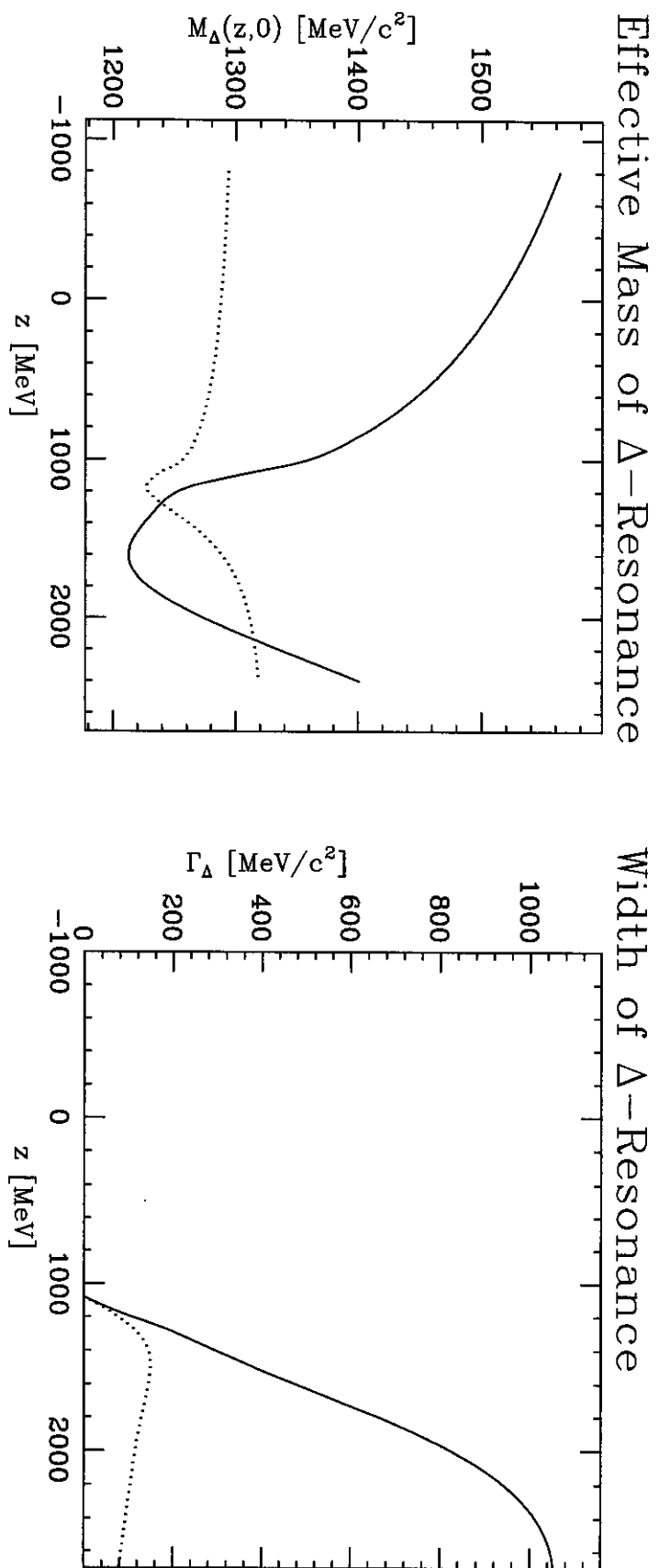


Fig 6, Kortemeyer, "The dynamical structure..."

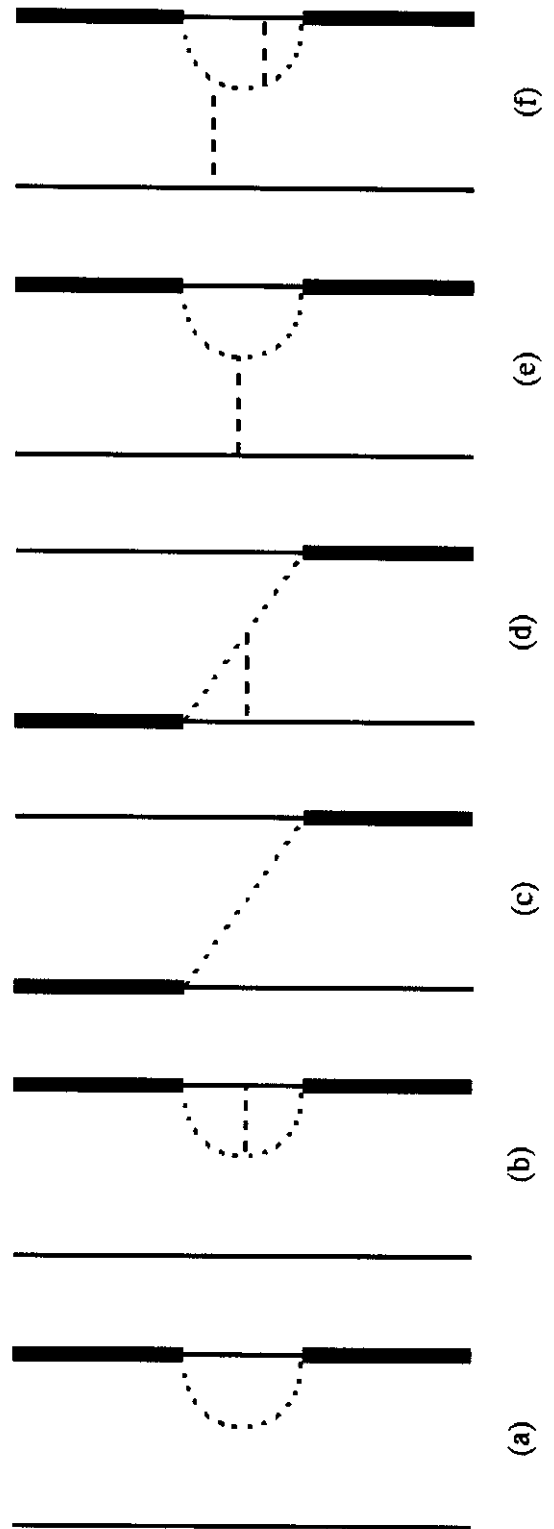
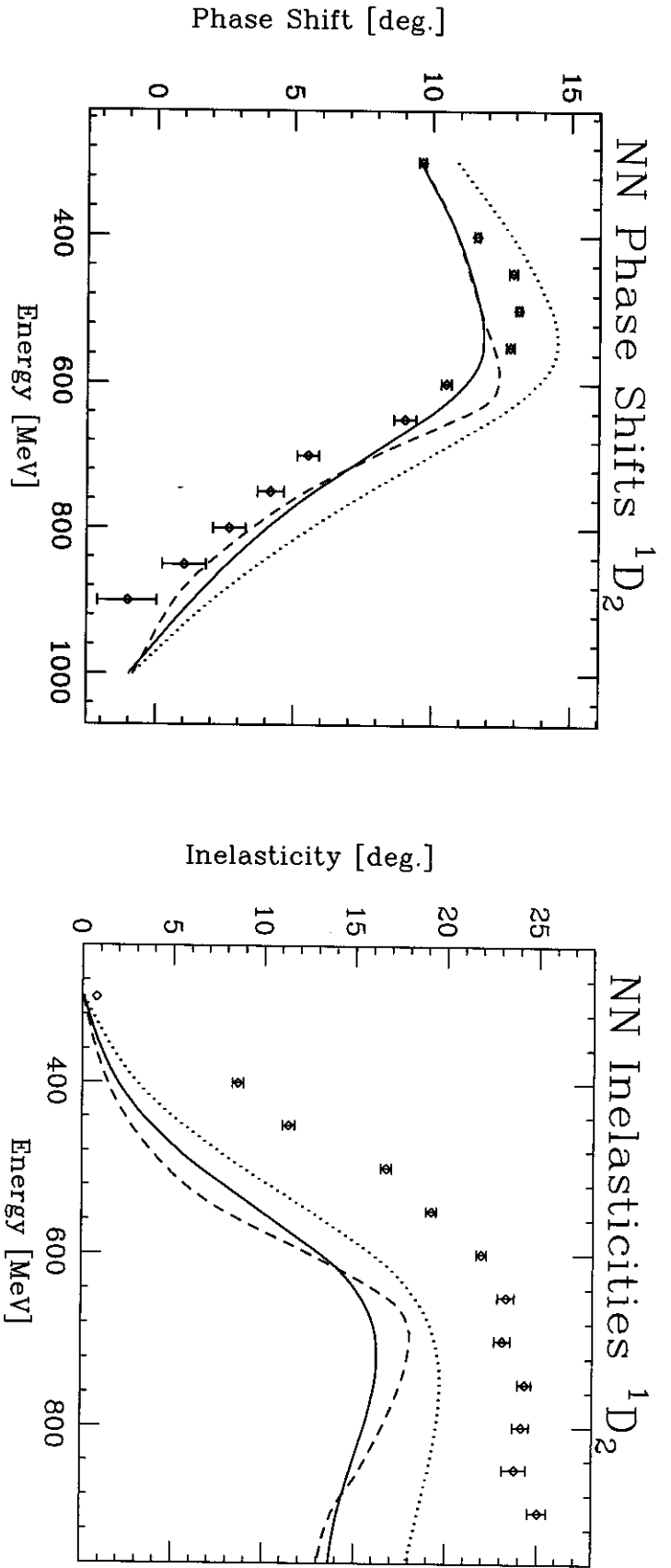
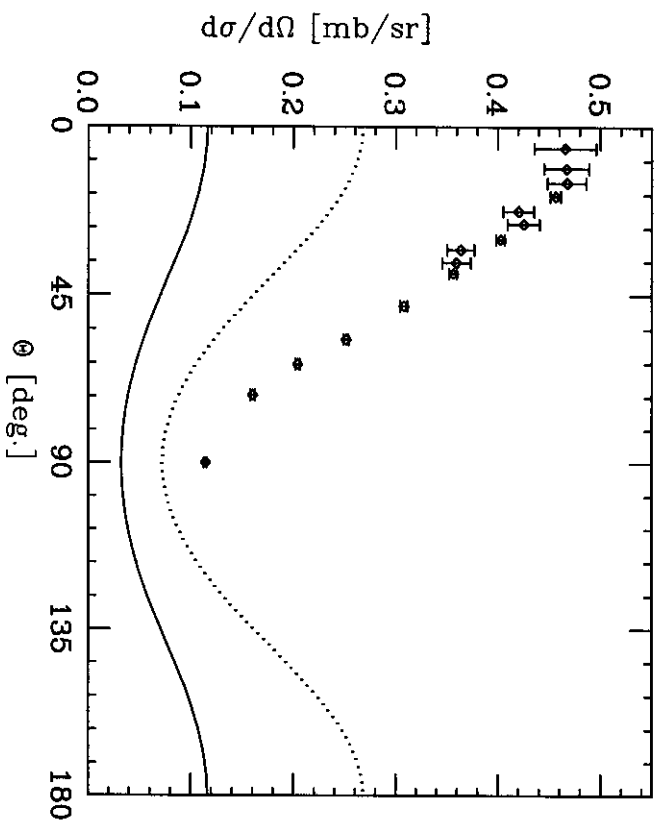


Fig 7, Kortemeyer,
"The dynamical structure..."



Diff. Cross Section $NN \rightarrow \pi d$ 578 MeV



Diff. Cross Section $NN \rightarrow \pi d$ 800 MeV

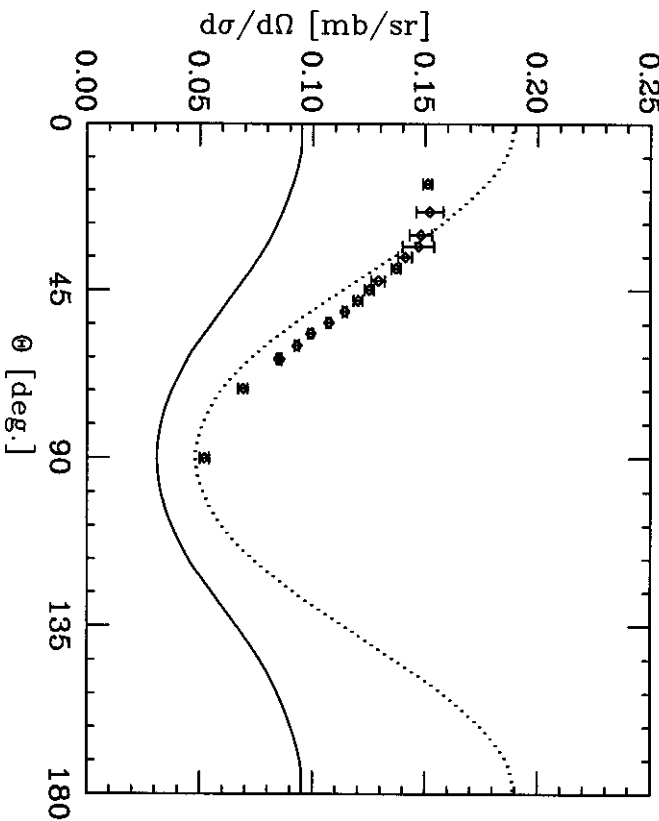


Fig 8, Kortemeyer,
"The dynamical struct."

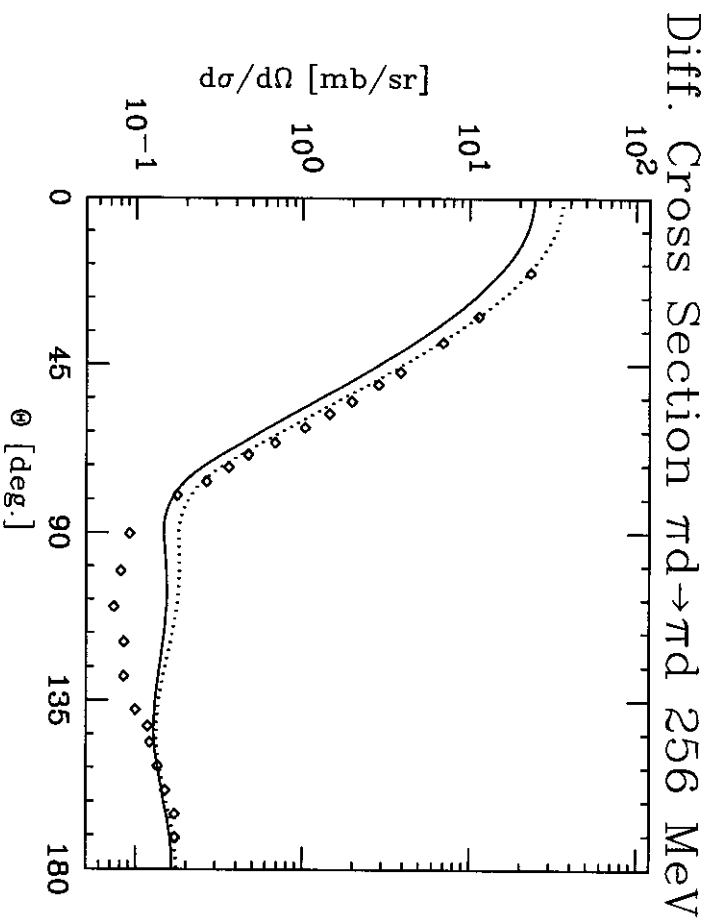
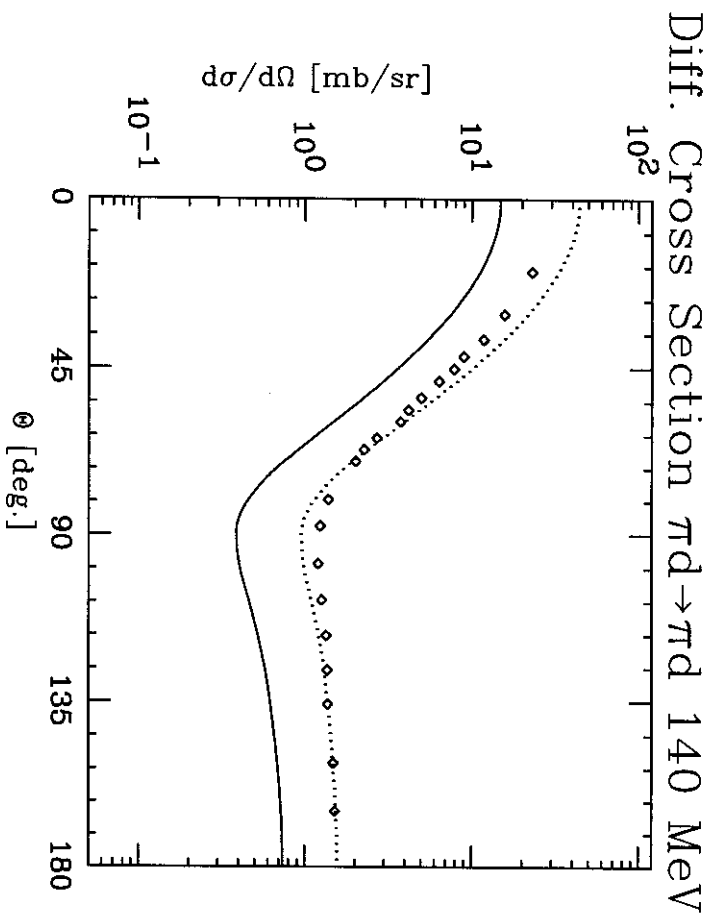


Fig 9, Kortemeyer,
"The dynamical struct."

Fig 10, Kortemeyer, "The dynamical struct."

